Available online at www.sciencedirect.com
ScienceDirect
Journal of Molecular Catalysis A: Chemical 279 (2008) 27–36
JOURNAL OF MOLECULAR CATALYSIS A: CHEMICAL
www.elsevier.com/locate/molcata

The isopropylation of biphenyl over one-dimensional zeolites with corrugated channels

Hiroyoshi Maekawa [a], Tomoko Shibata [a], Akita Niimi [a], Chiharu Asaoka [a], Kaori Yamasaki [a], Hiroaki Naiki [a], Kenichi Komura [a], Yoshihiro Kubota [a,1], Yoshihiro Sugi [a,*], Jae-Youl Lee [b], Jong-Ho Kim [b], Gon Seo [b]

[a] *Department of Materials Science and Technology, Faculty of Engineering, Gifu University, Gifu 501-1193, Japan*
[b] *School of Applied Chemical Engineering and The Research Institute for Catalysis, Chonnam National University, Gwangju 500-757, Republic of Korea*

Received 2 June 2007; received in revised form 13 September 2007; accepted 14 September 2007
Available online 29 September 2007

Abstract

The isopropylation of biphenyl (BP) was examined over one-dimensional zeolites with corrugated channels: SSZ-55 (ATS), SSZ-42 (IFR), L (LTL), and SSZ-35 (STF) zeolites, and compared to catalytic properties of H-mordenite (MOR). The selectivities for 4,4′-diisopropylbiphenyl (4,4′-DIPB) over these zeolites were in the range of 10–40%: they are much lower than that of MOR in spite of similar sizes of pore-entrance. These differences are due to the channel structures: they have larger reaction spaces due to one-dimensional corrugated channels compared to MOR with straight channels. The corrugated channels, even for STF, are too large for the selective formation of 4,4′-DIPB.

Keywords: SSZ-53; SSZ-42; L zeolite; SSZ-35; Mordenite; Corrugated channel; BP; Isopropylation; Shape-selectivity

1. Introduction

Large-pore molecular sieves (LPMS) are expected for useful catalysts in the alkylation of bulky polynuclear aromatics [1–4]. Highly dealuminated H-mordenite (MOR), which has straight channels with side pocket, gave 4,4′-diisopropylbiphenyl (4,4′-DIPB) from biphenyl (BP) with high activities and selectivities [1–7]. The selective formation of 4,4′-DIPB indicates that catalytically active sites on MOR effectively differentiate the least bulky 4,4′-DIPB from the other DIPB isomers at the transition states by the steric restriction in their channels.

Our previous relevant findings on the subjects were published on the alkylation of BP over SSZ-31 [8], SSZ-24 [9], SAPO-5 [10], and MAPO-5 (M: Mg, Ca, Sr, Ba, and Zn) [11], and CIT-5 [12] with straight channels. However, MAPO-36 (M: Mg and Zn) with ATS topology gave only the 30–35% selectivities for 4,4′-DIPB: predominant isomers were 2,*x*′-DIPB at lower temperatures, and 3,4′- and 3,3′-DIPB at higher temperatures [13,14]. MAPO-36 has corrugated channels with similar sized pore-entrances to MOR; however, no straight parts in their channels [15]. These results suggest that the selectivities for 4,4′-DIPB are influenced by the structure of channels.

SSZ-55, SSZ-42, and SSZ-35 zeolites are recently synthesized high silica molecular sieves having one-dimensional corrugated channels with no straight parts [15], and are expected to work as potential acid catalysts. SSZ-55 (topology: ATS) and SSZ-42 (topology: IFR) zeolites were synthesized as the borosilicates by the use of [(1-(3-fluorophenyl)cyclopentyl)methyl]trimethylammonium hydroxide [16–19], and *N*-benzyl-1,4-diazabicyclo[2.2.2]octane hydroxide, as structure-directing agents (SDA), respectively [20–23]. These two zeolites have twelve-membered (12-MR) pore-entrance with one-dimensional corrugated channels [15]. SSZ-35 zeolite (topology: STF), which has 10-MR pore-entrance with one-dimensional corrugated channels [15], was first synthesized by using SDA derived from 1,3,3,8,8-pentamethyl-3-azoniabicyclo[3.2.1]octane [24–27]. Recently, it was also synthesized by using *cis*,*cis*,*cis*-*N*-methylhexahydrojulolidinium hydroxide as SDA [28,29].

* Corresponding author.
E-mail address: sugi@apchem.gifu-u.ac.jp (Y. Sugi).
[1] Current address: Department of Materials Science and Engineering, Graduate School of Engineering, Yokohama National University, Yokohama 240-8501, Japan.

1381-1169/$ – see front matter © 2007 Elsevier B.V. All rights reserved.
doi:10.1016/j.molcata.2007.09.020

L Zeolite also have largest corrugated channels: 24-MR cages (topology: LTL. pore-entrance: 0.71 nm × 0.71 nm) [15].

The interests how channels of zeolites work in the isopropylation of BP encourage us to investigate the catalytic properties of the zeolites with corrugated channels. In this paper, we describe the isopropylation of BP over SSZ-55, SSZ-42, L, and SSZ-35 zeolites with ATS, IFR, LTL, and STF topologies, respectively, and compared to MOR, for the elucidation of the mechanism of the shape-selective catalysis in the zeolites.

2. Experimental

2.1. Zeolites

SSZ-55, SSZ-42, and SSZ-35 zeolites were synthesized according to the literatures [16,20,28]. SSZ-55 and SSZ-42 zeolites synthesized as borosilicates were aluminated with aqueous aluminum nitrate solution at 80 °C [19–21]. S1, S2, S3, and S4 indicate the numbers of the alumination of SSZ-55. SSZ-35 zeolite was also synthesized through its borosilicate using 6,10-dimethyl-5-azonia-spiro[4.5]decane hydroxide as SDA [27]. H-Mordenite and L zeolite were obtained from Tosoh Corporation (MOR: $SiO_2/Al_2O_3 = 128$; TSZ-690HOA. L: $SiO_2/Al_2O_3 = 6.1$; TSZ-500KOA). L Zeolite obtained as K-form was converted to H-form using 1M NH_3NO_3 aqueous solution.

The structures and properties of zeolites have been characterized by FE-SEM, XRD, ICP analysis, N_2 and *o*-xylene adsorption, NH_3-TPD, ^{27}Al and ^{29}Si MAS-NMR. Properties of these zeolites related to the catalysis are summarized in Table 1.

2.2. Isopropylation of BP

The alkylation of BP was carried out in a 100-mL SUS-316 autoclave under our standard conditions [7]. Catalyst (250 mg) and BP (7.7 g; 50 mmol) were placed in the autoclave, flushed with nitrogen, and heated to desired temperature (150–350 °C). Propene (0.8 MPa) was then introduced to the desired pressure, and agitated for 4 h. The pressure kept constant throughout the reaction. After cooling the autoclave, the products were separated from catalysts by filtration. The solution (*ca.* 1.5 mL) taken from the combined filtrate and washings was diluted with toluene (1.5–6.0 mL), and subjected to the analysis by a gas chromatography (GC-14A or GC-18A, Shimadzu Corporation) equipped with an Ultra-1 capillary column (25 m × 0.2 mm; Agilent Technologies). The products were also identified by a Shimadzu GC-MS 5000 gas chromatograph–mass spectrometer.

The yield of each product is calculated on the basis of the amounts of starting BP. The selectivities for diisopropylbiphenyl (DIPB) isomers are expressed based on total amounts of DIPB isomers.

The analysis of the encapsulated products in the catalyst used for the reaction was carried out as follows: the catalyst was separated by filtration, washed well with 200 mL of acetone, and dried at 110 °C for 12 h. The resulting catalyst (100 mg) was carefully dissolved using 3 mL of aqueous hydrofluoric acid (47%) at room temperature. This solution was neutralized with

Table 1
Properties of zeolites

Zeolite	FTC	Pore-entrance (MR)	Pore-entrance (nm)	Channels	Cage (MR)	SiO_2/Al_2O_3	Surface area (m^2/g)	External surface area (m^2/g)[a]	Pore volume (mL/g)	Peak temp. (°C)[b]	Acid amount (mmol/g)[b]
SSZ-55	ATS	12	0.65 × 0.75	Corrugated	20	73(S4)	466	16	0.2	305	0.31
						100(S3)	468	18	0.2	299	0.26
						160(S2)	478	18	0.19	299	0.12
						306(S1)	417	11	0.17	284	0.04
SSZ-42	IFR	12	0.62 × 0.72	Corrugated	24	280	518	11	0.20	255	0.08
SSZ-35	STF	10	0.54 × 0.57	Corrugated	18	45	328	8.7	0.11	273	0.66
Mordenite	MOR	12	0.65 × 0.70	Straight with 8-MR side pocket	–	128	460	35	0.16	389	0.20
L	LTL	12	0.71 × 0.71	Corrugated	24	6.1	253	33	0.58	403	0.88

[a] Calculated from *t*-plot of N_2 adsorption.
[b] Calculated from NH_3-TPD profiles.

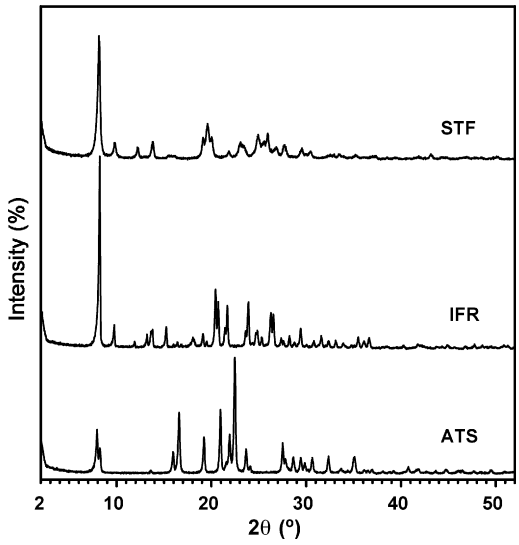

Fig. 1. XRD patterns of calcined SSZ-55, SSZ-42, and SSZ-35 zeolites.

solid potassium carbonate, and the organic layer was extracted three times with 20 mL of dichloromethane. After removal of the solvent *in vacuo*, the residue was dissolved in 5 mL of toluene, and then, analyzed according to the procedure that has been used for the bulk products. The selectivities for DIPB isomers in encapsulated products were defined in a similar manner as those in the bulk products. The selectivity for the products in the encapsulated products was expressed by the composition of reaction mixtures because it is difficult for the quantitative analyses.

2.3. Characterization of the Catalysts

The crystal structure of zeolites were determined by powder X-ray diffraction using a Shimadzu XRD-6000 diffractometer with Cu Kα radiation (λ = 1.5418 Å). Elemental analysis was performed by inductive coupled plasma atomic emission spectroscopy on a JICP-PS-1000 UV spectrometer (Teledyne Leeman Labs Inc.). Crystal size and morphology of the sample were determined by an S-4300 FE-SEM microscope (Hitachi Corporation). Nitrogen adsorption measurements were carried out on a Belsorp 28SA apparatus (Bel Japan Inc.). The adsorption of *o*-xylene was performed by gravimetric method with its vapor (0.48 kPa) using a highly sensitive quartz microbalance at 120 °C after the evacuation at 550 °C. Ammonia temperature programmed desorption (NH_3-TPD) was measured using a Bel TPD-66 apparatus: the catalyst was evacuated at 400 °C for 1 h, and ammonia was adsorbed at 100 °C followed by further evacuation for 1 h. Then, the sample was heated from 100 to 710 °C at the rate of 10 °C/min in a helium stream. ^{27}Al spectra of zeolites were recorded at room temperature under magic angle spinning (MAS) by using 4 mm diameter zirconia rotors spinning at 15 kHz on a ECA-500 NMR (JEOL Ltd.), and ^{29}Si NMR by using 7.0 mm diameter zirconia rotors spinning at 5 kHz on a Unity Solid Inova WB 200 MHz System (Varian Corporation).

3. Results and discussion

3.1. Properties of zeolites

Typical physico-chemical properties of the zeolites, SSZ-55, SSZ-42, SSZ-35, MOR, and L zeolites used for the isopropylation of BP were shown in Table 1. These properties are compatible for the zeolites in the literatures [15,19,23,28].

Fig. 1 shows the XRD patterns of calcined SSZ-55, SSZ-42, and SSZ-35 zeolites. Their patterns were identical with those described in the literatures [15,19,23,28]. Fig. 2 shows the typical SEM images of the as-synthesized samples.

The substitution of B^{3+} in [B]-SSZ-55 and [B]-SSZ-42 with Al^{3+} was carried out by using 1 M $Al(NO_3)_3$ solution at 80 °C according to the literatures [19–21]. XRD patterns of resultant zeolites were almost identical after repeating the substitution for three times. These observations suggest that no collapse of the structure occurs during the calcination and the substitution of B^{3+} with Al^{3+}.

N_2 adsorption of SSZ-55, SSZ-42, and SSZ-35 zeolites shows typical type-I isotherm (see Fig. 1 Supplementary data). Specific surface area and pore volume were 420–520 m^2/g and 0.15–0.20 mL/g, respectively. These results indicate that SSZ-55, SSZ-42, and SSZ-35 zeolites have typical microporous nature. External surface areas calculated from *t*-plot of N_2 adsorption were 38, 11, and 8.7 m^2/g for SSZ-55, SSZ-42, and SSZ-35 zeolites, respectively.

Fig. 3 shows the adsorption of *o*-xylene on MOR, SSZ-55, SSZ-42, MOR, L, and SSZ-35 zeolites. *o*-Xylene rapidly adsorbed over SSZ-55, SSZ-42, MOR, and L zeolites, and the amounts were saturated in short periods. The initial rate of adsorption are 9.2 mg/(g min) for SSZ-42, 6.2 mg/(g min)

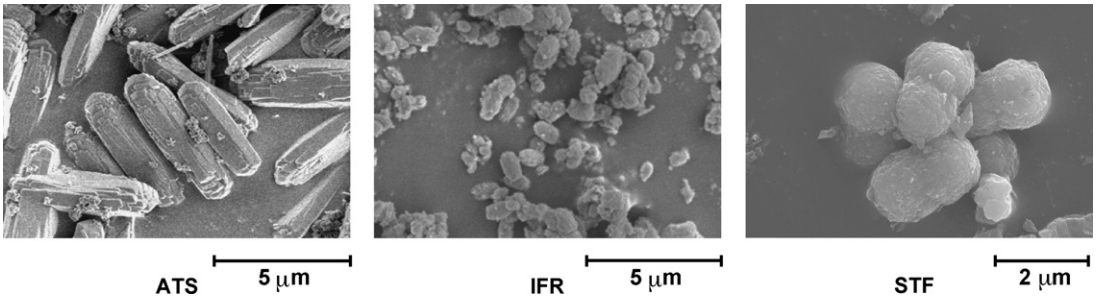

Fig. 2. SEM Images of as-synthesized SSZ-55, SSZ-42, and SSZ-35 zeolites.

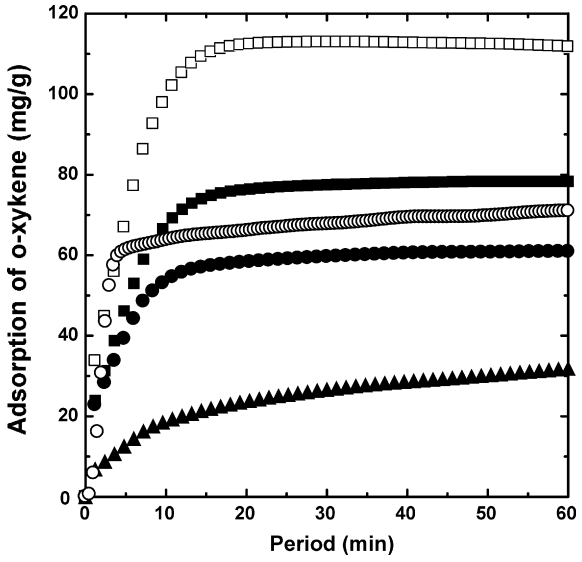

Fig. 3. *o*-Xylene adsorption on SSZ-55 (S2), SSZ-42, and SSZ-35 zeolites. (■) SSZ-55; (□) SSZ-42; (●) MOR; (○) L; (▲) SSZ-35.

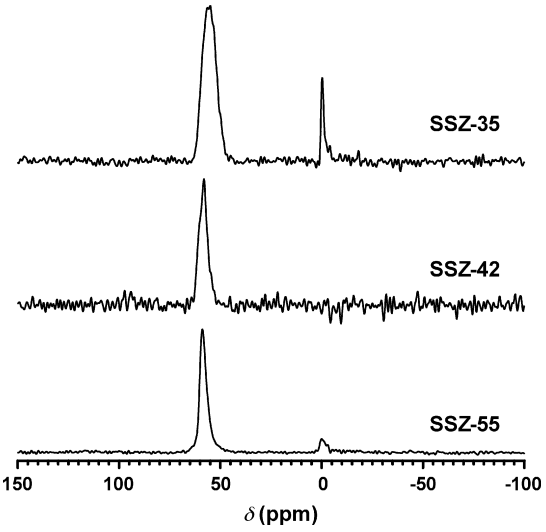

Fig. 4. ^{27}Al MAS NMR spectra of SSZ-55 (S2), SSZ-42, and SSZ-35 zeolites.

for SSZ-55, 4.6 mg/(g min) for MOR, and 15.5 mg/(g min) for L zeolite, and total adsorption amounts after 60 min were 112 mg/g for SSZ-42, 78 mg/g for SSZ-55, 61 mg/g for MOR, and 71 mg/g for L zeolite. It means that their channels are large enough for the diffusion of *o*-xylene in them. Particularly, rapid adsorption on SSZ-42 and L zeolites may be due to large pore-entrance and channels. However, SSZ-35 adsorbed with initial rate of 1.6 mg/(g min), and amounts of the adsorption after 60 min was 31.9 mg/g, which are much slower than those of SSZ-55, SSZ-42, and MOR. These results means that SSZ-35 has smaller pore-entrance than MOR, SSZ-55, SSZ-42, and L zeolites. From these adsorption of *o*-xylene, the pore-entrances of SSZ-55, SSZ-42, MOR, and L zeolites are enough for entering BP and its products in their channels, particularly, SSZ-55, SSZ-42, and L zeolites have larger spaces in their channels than MOR has. However, the pore-entrances of SSZ-35 is not so large for the adsorption of *o*-xylene, and it is relatively severe for BP and its isopropylates to enter in the zeolite.

^{27}Al MAS NMR spectra of calcined SSZ-55, SSZ-42, and SSZ-35 zeolites, are shown in Fig. 4. Peaks at around 50 ppm observed in ^{27}Al NMR spectra of all zeolites are assigned to tetrahedral Al^{3+} species which are incorporated to zeolite framework. However, SSZ-35 zeolite had also relatively large Al^{3+} peaks at around 0 ppm assigned to octahedral Al^{3+} species which are not incorporated in the framework. Similar octahedral Al^{3+} species also appeared by the substitution of B^{3+} in the frameworks of [B]-SSZ-55 and [B]-SSZ-42 with Al^{3+}. These tetrahedral Al^{3+} species work as Brønsted acidic sites related to the catalytic activity in the solid acid catalysis. Small Q^3 species was observed near Q^4 species in ^{29}Si MAS NMR spectra of all zeolites (see Fig. 2 in Supplementary data). The peak sizes of Q^3 species were roughly corresponding to SiO_2/Al_2O_3 ratio of the zeolites.

TPD profiles of SSZ-55, SSZ-42, and SSZ-35, MOR, and L zeolites are shown in Fig. 5. They have two peaks, *l*- and *h*-peaks at around 150–200 °C and 230–450 °C, respectively. The *l*-peaks are due to physical adsorption of NH_3, and the *h*-peaks are assigned to NH_3 desorbed from Brønsted acid sites which are related to active sites in solid acid catalysis. The peak temperature for *h*-peak is the highest for MOR, and decreased in the order: L≈MOR ≫ SSZ-35 ≥ SSZ-55 > SSZ-42. The order corresponds to the order of acid strength (see Table 1). Acid amounts, calculated from area of deconvoluted *h*-peak, correspond to the SiO_2/Al_2O_3 ratio (see Table 1). These zeolites have weaker acidities than MOR and L zeolites, particularly, SSZ-42 zeolite has the lowest acidity among five zeolites; however, their acidities are enough for the solid acid catalysis, such as the isopropylation of BP.

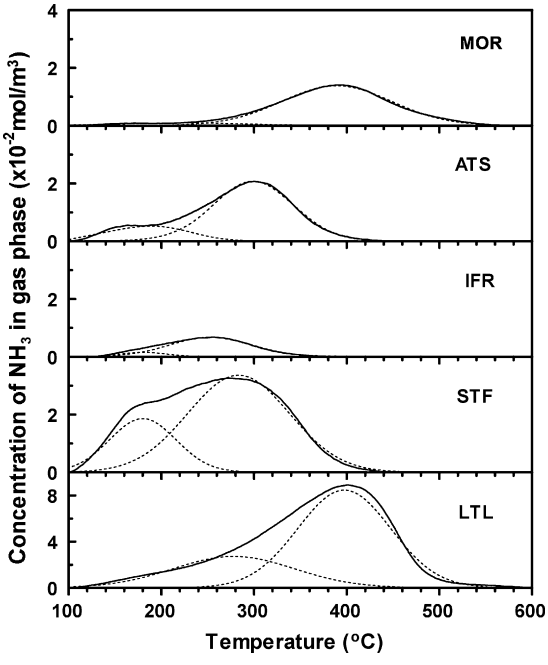

Fig. 5. NH_3-TPD profiles of MOR, SSZ-55 (S2), SSZ-42, and SSZ-35 zeolites.

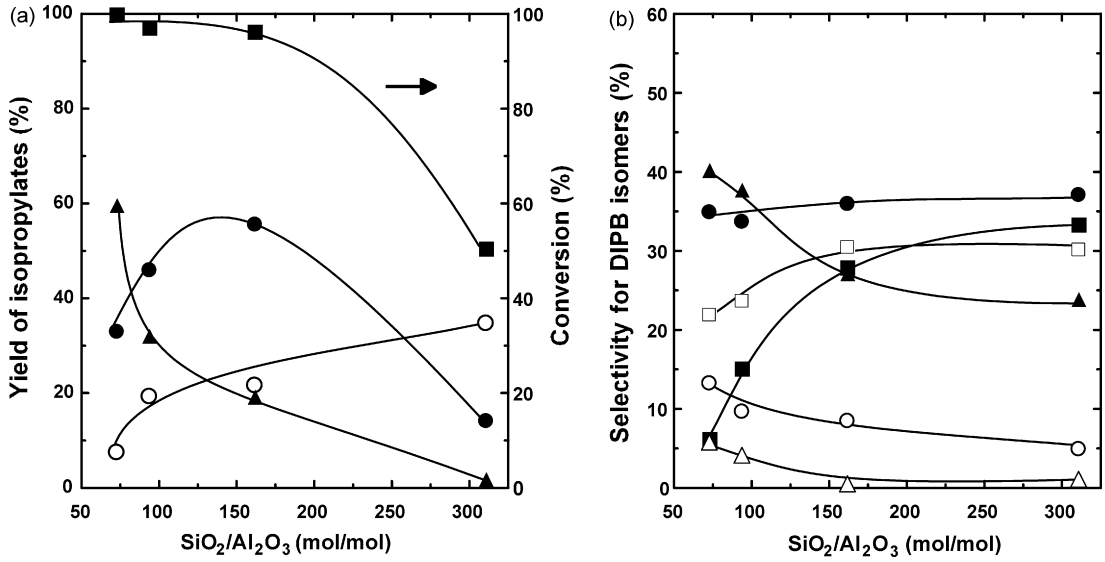

Fig. 6. The influence of SiO_2/Al_2O_3 ratio on the isopropylation of BP over SSZ-55 zeolite. (a) Yield of isopropylates. (b) Selectivity for DIPB isomers. Reaction conditions: BP, 25 mmol; catalyst, SSZ-55 (SiO_2/Al_2O_3 = 73–306), 0.125 g; temperature, 250 °C; propene, pressure, 0.8 MPa; time, 4 h. *Legends*: (a) (■) conversion; (◯) IPBP isomers; (●) DIPB isomers; (▲) TriIPB isomers. (b) Bulk products: (■) 4,4′-DIPB; (●) 3,4′-DIPB; (◯) 3,3′-DIPB; (▲) 2,*x*′-DIPB; (△) 3,5-DIPB. Encapsulated product: (□) 4,4′-DIPB.

3.2. The isopropylation of BP

3.2.1. SSZ-55 zeolite

Fig. 6 shows the influence of SiO_2/Al_2O_3 ratio on the isopropylation of BP over SSZ-55 zeolite at 250 °C. The conversion of BP decreased with increasing the ratio as shown in Fig. 6a. The yield of DIPB isomers first increased with increasing the ratio, reached maximum at the ratio of *ca*. 150, and then, it decreased with further increase in the ratio. However, the yield of isopropylbiphenyl (IPBP) isomers increased with the increase in the ratio, accompanying the decrease in the yield of triisopropylbiphenyl (TriIPB) isomers.

The influence of SiO_2/Al_2O_3 ratio on the selectivity for DIPB isomers is shown in Fig. 6b. The selectivities for 4,4′-DIPB in bulk products increased with the increase in the SiO_2/Al_2O_3 ratio from 5% at 75 to 30% at 306. The increase in the selectivities for 4,4′-DIPB was accompanied by the decrease in those for 2,*x*′- (sum of 2,2′-, 2,3′-, and 2,4′-), 3,3′-, and 3,5-DIPB; however, the selectivities for 3,4′-DIPB were almost constant. The selectivities for 4,4′-DIPB in encapsulated products also increased with the increase in the ratios. These lower selectivities for 4,4′-DIPB over SSZ-55 with the low SiO_2/Al_2O_3 ratio are due to the non-selective reactions, such as the alkylation and the isomerization at the external acid sites. However, there are possibilities of the isomerization of 4,4′-DIPB inside the channels. The predominant formation of 2,*x*′- and 3,4′-DIPB at SiO_2/Al_2O_3 = 306 suggests that the channels are too large to exclude the bulky DIPB isomers at their transition states from the SSZ-55 channels to allow their formation in them.

The selectivity for 4,4′-DIPB in the level of 30% at SiO_2/Al_2O_3 = 306 is higher than the value in the equilibrium of DIPB isomers. This suggests that SSZ-55 channels have some shape-selective nature in the isopropylation of BP although the formation of bulkier isomers cannot be prevented.

Fig. 7 shows the influence of reaction temperature on the isopropylation of BP over SSZ-55 zeolite with SiO_2/Al_2O_3 = 306. The conversion of BP and the yields of IPBP, DIPB, and TriIPB isomers increased with increasing the temperatures (Fig. 7a). IPBP isomers were principal products at lower temperatures, and the yield of DIPB isomers increased much at the temperatures higher than 300 °C.

The selectivities for DIPB isomers in both bulk and encapsulated products are shown in Fig. 7b. The selectivity for 4,4′-DIPB in bulk products was around 35% below 350 °C; however, decreased to 15% at 350 °C. The selectivities for 4,4′-DIPB in encapsulated products were 28–35% in the range of 150–350 °C. The selectivities for 2,*x*′-DIPB decreased from 32% at 200 °C to 10% at 350 °C, and the selectivities for other isomers increased from 30% at 200 °C to 50% at 350 °C for 3,4′-DIPB and 4% at 200 °C to 20% at 350 °C for 3,3′-DIPB. These results also indicate that SSZ-55 zeolite has some shape-selective nature in the isopropylation of BP because the selectivities for 4,4′-DIPB at the moderate temperatures are higher than equilibrium composition of 4,4′-DIPB [30]. The selectivity levels of around 30% means that the bulky 2,*x*′-, 3,4′- and 3,3′-DIPB cannot be excluded completely at their transition states by the steric restriction in the SSZ-55 channels, because the channels are too loose to form selectively the slimmest 4,4′-DIPB.

The predominant formation of bulky 2,*x*′-DIPB at low temperatures means that the participation of kinetic control: electron-rich 2-position is preferentially attacked to yield 2,*x*′-DIPB. The decrease in the selectivities for 2,*x*′-DIPB with the increase in the temperatures means the participation of thermodynamic control, resulting in the increase in the formation of thermodynamically stable 3,4′- and 3,3′-DIPB.

Similar levels of the selectivities for 4,4′-DIPB were observed in the isopropylation of BP over MAPO-36 (M: Mg and Zn) with ATS topology [14,15]. These results show that the selectivity for

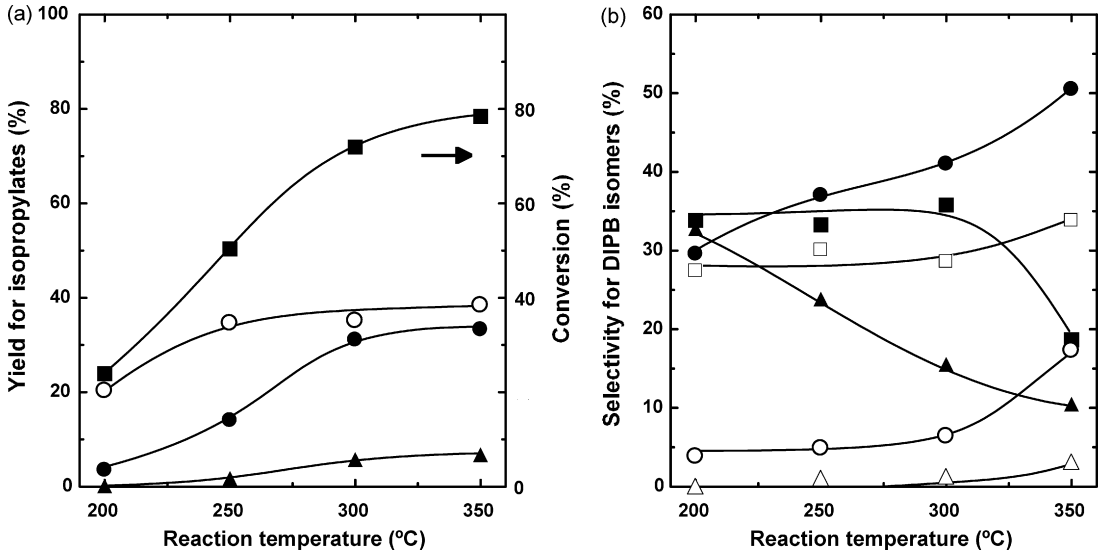

Fig. 7. The influence of reaction temperature on the isopropylation of BP over SSZ-55 zeolite. (a) Yield of isopropylates. (b) Selectivity for DIPB isomers. Reaction conditions: BP, 25 mmol; catalyst, SSZ-55 ($SiO_2/Al_2O_3 = 306$), 0.125 g; temperature, 200–350 °C; propene, pressure, 0.8 MPa; time, 4 h. *Legends*: (a) (■) conversion; (◯) IPBP isomers; (●) DIPB isomers; (▲) TriIPB isomers. (b) Bulk products: (■) 4,4′-DIPB; (●) 3,4′-DIPB; (◯) 3,3′-DIPB; (▲) 2,*x*′-DIPB; (△) 3,5-DIPB. Encapsulated product: (□) 4,4′-DIPB.

4,4′-DIPB over zeolites with ATS topology was controlled by the size of pore-entrance and shapes of channels, and not by the type of metal species: Si, Mg, and Zn. Similar phenomena were also observed for SSZ-24 and MAPO-5 (M: Si, Mg, Ca, Sr, Ba, and Zn) with AFI topology [11].

3.2.2. SSZ-42 zeolite

Fig. 8 shows the influence of temperature on the isopropylation of BP over SSZ-42 zeolite. The selectivities for 4,4′-DIPB were *ca*. 35% among DIPB isomers at 200 °C, and decreased to 20% at 350 °C. The selectivity for 2,*x*′-DIPB isomers were also *ca*. 35% at 200 °C and decreased to less than 10% at 350 °C. Corresponding to the decreases in the selectivities for these bulky and thermodynamically unstable isomers, the selectivities for the thermodynamically stable 3,4′- and 3,3′-DIPB increased with increasing the reaction temperature: *ca*. 20% at 200 °C to 40% at 350 °C for 3,4′-DIPB and 10% at 200 °C to 25% at 300 °C for 3,3′-DIPB. These results resemble the results obtained over SSZ-55, and show that the steric restriction at the transition states was not effectively operated in the isopropylation: the catalysis occurs principally by the kinetic control at lower temperatures, and the thermodynamic control becomes predominant with increasing the temperature.

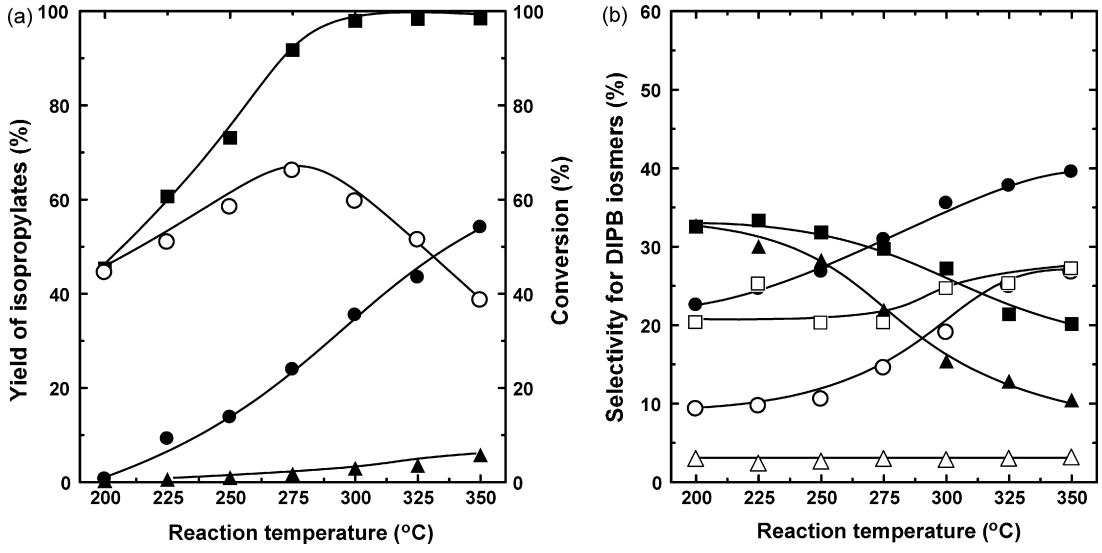

Fig. 8. The influence of reaction temperature on the isopropylation of BP over SSZ-42 zeolite. (a) Yield of isopropylates. (b) Selectivity for DIPB isomers. Reaction conditions: BP, 50 mmol; catalyst, SSZ-42 ($SiO_2/Al_2O_3 = 280$), 0.25 g; temperature, 200–350 °C; propene, pressure, 0.8 MPa; time, 4 h. *Legends*: (a) (■) conversion; (◯) IPBP isomers; (●) DIPB isomers; (▲) TriIPB isomers. (b) Bulk products: (■) 4,4′-DIPB; (●) 3,4′-DIPB; (◯) 3,3′-DIPB; (▲) 2,*x*′-DIPB; (△) 3,5-DIPB. Encapsulated product: (□) 4,4′-DIPB.

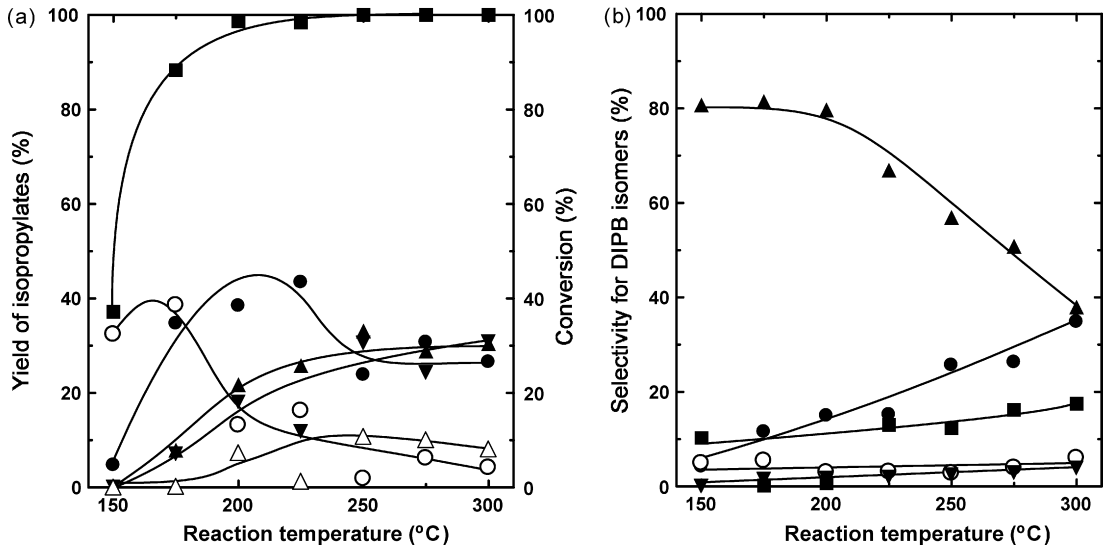

Fig. 9. The influence of reaction temperature on the isopropylation of BP over L zeolite. (a) Yield of isopropylates. (b) Selectivity for DIPB isomers. Reaction conditions: BP, 50 mmol; catalyst, L zeolite (SiO_2/Al_2O_3 = 6.1), 0.25 g; temperature, 150–300 °C; propene, pressure, 0.8 MPa; time, 4 h. *Legends*: (a) (■) conversion; (◯) IPBP isomers; (●) DIPB isomers; (▲) TIPB isomers; (▼) TetraIPB isomers; (△) Penta-IPB. (b) Bulk products: (■) 4,4′-DIPB; (●) 3,4′-DIPB; (◯) 3,3′-DIPB; (▲) 2,*x*′-DIPB; (△) 3,5-DIPB.

The selectivities for 4,4′-DIPB in the encapsulated products were around 20% at 200–275 °C, as shown in Fig. 8b; however, increased to 25% at 350 °C. The selectivities for 4,4′-DIPB were higher than the composition of the DIPB isomer in equilibrium at the corresponding conditions. As discussed for SSZ-55, the SSZ-42 channels have some shape-selective nature in the isopropylation of BP although they are too large for the selective formation of 4,4′-DIPB. The preferential formation of 2,*x*′-DIPB at lower temperatures and of a thermodynamically more stable isomer, 3,4′-DIPB at higher temperatures indicates that the steric restriction for the formation of DIPB isomers with the pores is loose for the shape-selective formation of 4,4′-DIPB even if the steric restriction of bulky isomers with the pores is effectively operating as described for SSZ-55 in the previous sections.

3.2.3. L *zeolite*

Fig. 9 shows the influence of reaction temperature on the isopropylation of BP over L zeolite. The catalytic activities were very high even at low temperatures as shown in Fig. 9a. The yield of DIPB isomers increased with the temperatures, and the formation of TriIPB, TetraIPB, and PentaIPB isomers were enhanced with further increase in the temperature. These results of L zeolite resemble those of Y zeolite with large reaction spaces inside the channels [31].

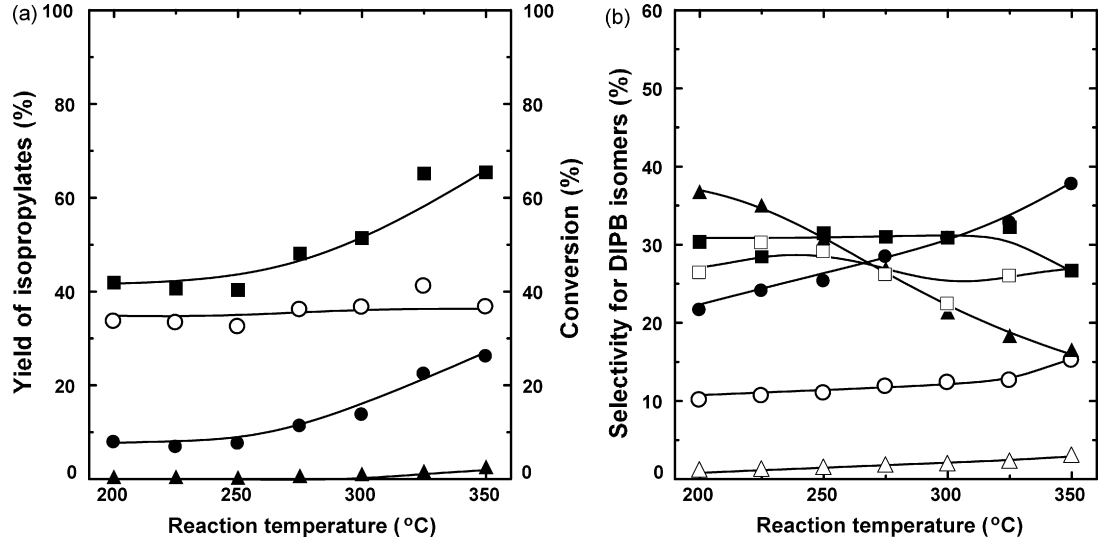

Fig. 10. The influence of reaction temperature on the isopropylation of BP over SSZ-35 zeolite. (a) Yield of isopropylates. (b) Selectivity for DIPB isomers. Reaction conditions: BP, 50 mmol; catalyst, SSZ-35 (SiO_2/Al_2O_3 = 45), 0.25 g; temperature, 200–350 °C; propene, pressure, 0.8 MPa; time, 4 h. *Legends*: (a) (■) conversion; (◯) IPBP isomers; (●) DIPB isomers; (▲) TriIPB isomers. (b) Bulk products: (■) 4,4′-DIPB; (●) 3,4′-DIPB; (◯) 3,3′-DIPB; (▲) 2,*x*′-DIPB; (△) 3,5-DIPB. Encapsulated product: (□) 4,4′-DIPB.

The formation of 2,x'-DIPB isomers was highly significant at low temperatures, and thus, the selectivities for the other isomers, 4,4′-, 3,4′-, 3,3′-, and 3,5-DIPB were obtained only in low selectivities (Fig. 9b). The selectivity for 2,x'-DIPB decreased with the increase in the reaction temperatures, whereas the other isomers, particularly, 3,4′-DIPB, gradually increased with reaction temperatures, and the selectivity for 4,4′-DIPB was less than 15% at all temperatures. These results show that the kinetic control was primarily operated in the isopropylation of BP at lower temperatures, and that the reaction was predominantly controlled by thermodynamic factors at higher temperatures. These features of the catalysis over L zeolite suggest that their channels have no shape-selective nature in the isopropylation of BP because they are too large for the selective formation of 4,4′-DIPB.

3.2.4. SSZ-35 zeolite

Fig. 10 shows the influence of reaction temperature on the isopropylation of BP over SSZ-35 zeolite. The SSZ-35 zeolite had considerably high catalytic activity: principal products were IPBP isomers in 30–35% yield in the range of 200–350 °C, and the yield of DIPB increased gradually with increasing the temperature. The selectivities for 4,4′-DIPB were 30% for bulk products and 20–30% for encapsulated product in the range of 200–325 °C. The selectivity for 2,x'-DIPB decreased with the increase in the temperature accompanying the increase in the selectivity for 3,4′-DIPB. On the other hand, the selectivities for 3,3′- and 3,5-DIPB were almost constant in the temperature range. The SSZ-35 zeolite obtained by the alumination of the borosilicate [27] also gave the similar level of the selectivity for 4,4′-DIPB [32].

It is unexpected for us that SSZ-35 zeolite has high catalytic activities and low DIPB selectivities in the isopropylation of BP in spite of its small 10-MR pore-entrances. We examined the isopropylation of 4,4′-DIPB over SSZ-35 zeolite to elucidate how the zeolite works in the isopropylation of BP. Fig. 11 shows the influence of reaction temperature on the isopropylation of 4,4′-DIPB. The conversion of 4,4′-DIPB was less than 10% even at 350 °C in spite of high acid amounts of SSZ-35 zeolite. The principal reactions were the isopropylation to TriIPB isomers and the de-alkylation to IPBP isomers; however, the isomerization of 4,4′-DIPB was not significant even at 350 °C. These results mean that the acid sites of SSZ-35 zeolite are not actually active for the isopropylation and the isomerization of 4,4′-DIPB, and strongly support that the isopropylation of BP over SSZ-35 zeolite occur inside the channels. The low selectivities for 4,4′-DIPB were due to the reactions in corrugated channels with 18-MR cavities of the zeolite. These results indicate that the channels of SSZ-35 zeolite are too large for the selective formation of 4,4′-DIPB.

The selectivities for 4,4′-DIPB in the level of 30% for bulk and encapsulated products show that SSZ-35 channels have some shape-selective nature as discussed for SSZ-55 and SSZ-42 zeolites. However, their restriction by corrugated channels is too loose to form selectively 4,4′-DIPB. Even the smallest pore-entrance of SSZ-35 among the zeolites in this study scarcely plays important roles for the shape-selective formation of 4,4′-DIPB, and allow the formation and diffusion of the other bulkier isomers, resulting in the low selectivities for 4,4′-DIPB.

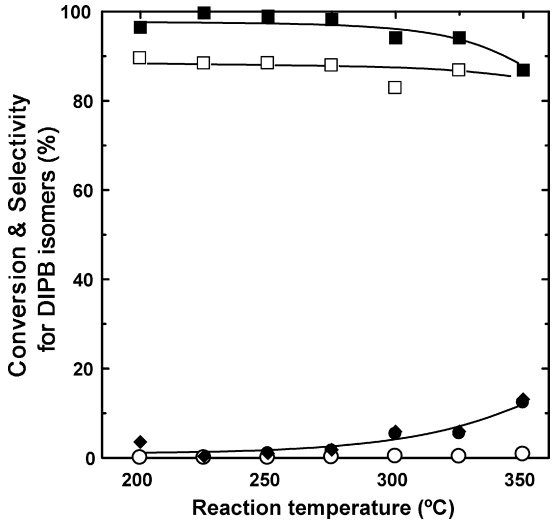

Fig. 11. The influence of reaction temperature on the isopropylation of 4,4′-DIPB over SSZ-35 zeolite. Reaction conditions: 4,4′-DIPB, 12.5 mmol; catalyst, SSZ-35 ($SiO_2/Al_2O_3 = 45$), 0.125 g; temperature, 200–350 °C; propene pressure, 0.8 MPa; time, 4 h. *Legends*: (■) 4,4′-DIPB; (●) 3,4′-DIPB; (◯) 3,3′-DIPB. Encapsulated product: (□) 4,4′-DIPB.

3.3. Catalysis over zeolites with corrugated channels

We previously found that MOR gave selectively 4,4′-DIPB among DIPB isomers in the isopropylation of BP: this is due to the shape-selective formation of the least bulky isomers by the exclusion of the transition states to the bulkier isomers. Similar restriction on transition state also works for large pore zeolites with straight channel such as SSZ-31 [8], SSZ-24 (topology: AFI) [9], SAPO-5 (topology: AFI) [10], and MAPO-5 (M: Mg and Zn; AFI) [11] with 12-MR pore-entrance, CIT-5 (topology: CFI) with 14-MR pore-entrance [13]. On the other hand, the selectivities for 4,4′-DIPB by the zeolites with corrugated channels, SSZ-55 and SSZ-42 zeolites with 12-MR pore-entrances and SSZ-35 zeolite with 10-MR pore-entrances were lower than those for MOR and other zeolites listed above.

These differences in the selectivities for 4,4′-DIPB are considered to the differences in channel structures of the zeolites because they have similar sized pore-entrances. SSZ-24 zeolites have the 12-MR straight channels: pore-entrance: 0.73 nm × 0.73 nm. Although MOR has 12-MR channels with side pockets (8-MR channels) (pore-entrance: 0.65 nm × 0.72 nm), MOR is considered to have the actually straight channels because the side pockets are small enough for access and accommodation of DIPB isomers. Although the selectivities for the DIPB isomers depend on the type of the zeolites, the isopropylation of BP is considered in the channels by restricted transition state mechanism, and the selectivity for 4,4′-DIPB is determined by the exclusion of bulky DIPB isomers due to the steric restriction inside the channels. MOR channels give the most appropriate channels for the exclusion of the transition states of bulky DIPB isomers, resulting in highly shape-

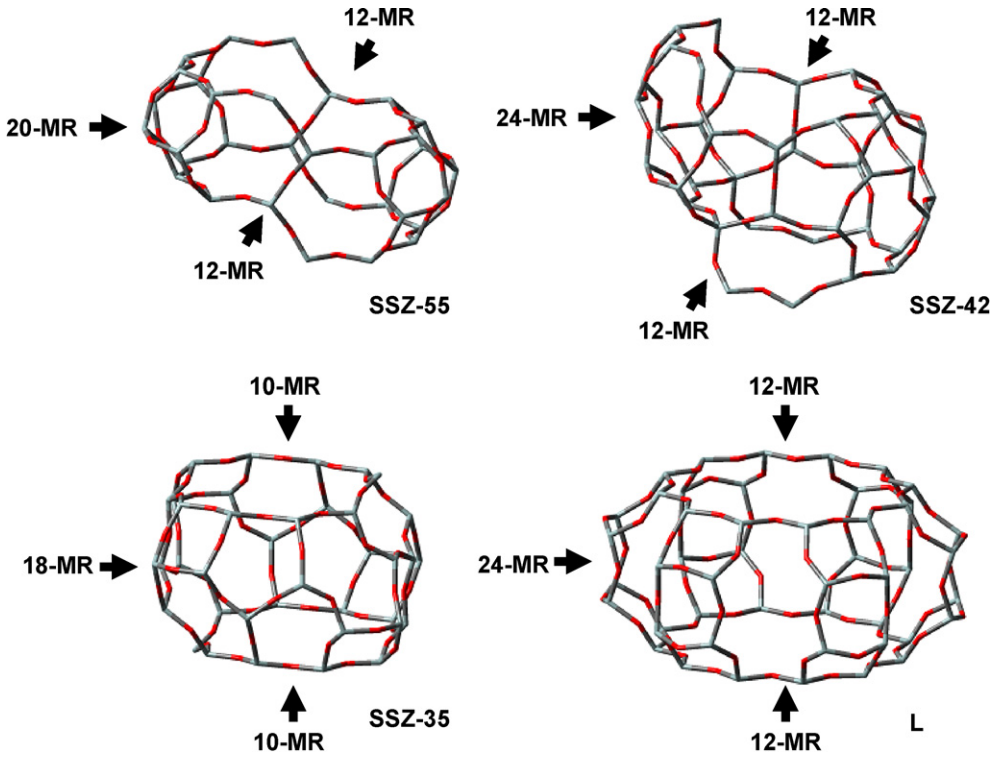

Fig. 12. Model of cages of corrugated zeolites.

selective formation of 4,4′-DIPB as proposed in the previous papers [1–7].

The zeolites with ATS, IFR, and LTL topologies have corrugated channels with cages [15]: ATS: 20-MR cages with 12-MR pore-entrance (0.65 nm × 0.75 nm), IFR: 24-MR cages with 12-MR pore-entrance (0.62 nm × 0.72 nm), and LTL: 24-MR cages with 12-MR pore-entrance (0.71 nm × 0.72 nm) as shown in Fig. 12, which are prepared based on the crystal data by International Zeolite Association [15]. These corrugated channels of the latter zeolites afford larger reaction spaces than the straight channels of the former zeolite although the zeolites listed have similar sized pore-entrances. These features of zeolites suggest that the differences in the selectivity for 4,4′-DIPB between straight and corrugated 12-MR zeolites are due to the differences in reaction spaces inside their channels. The corrugated channels of these zeolites cannot effectively exclude the transition states to yield the bulky DIPB isomers, and they are too large for the shape-selective isopropylation of BP, even for STF channels. These differences in the catalytic properties among ATS, IFR, LTL, and MOR are supported by the differences in the amount and rate of the adsorption of *o*-xylene. The low selectivity for 4,4′-DIPB was consistently observed in the isopropylation of BP over 14-MR zeolites, such as UTD-1 and SSZ-53 [32].

The selectivities for 4,4′-DIPB in the level of 25–35% over SSZ-55, SSZ-42, and SSZ-35 zeolites at moderate temperatures are higher than the equilibrium composition of 4,4′-DIPB at corresponding temperatures [30]. These results mean that the channels have some shape-selective nature in the isopropylation of BP although they are too large for the selective formation of 4,4′-DIPB, and that the formation of bulkier transition states for the other isomers, such as 3,3′- and 3,4′-DIPB, is also allowed inside their channels. However, L zeolite have no shape-selective nature for the isopropylation of BP, and thus, it gave only the low selectivity in less than 15% at all temperatures.

The selectivity for 4,4′-DIPB was in the level of 30–40% in the isopropylation of BP over SSZ-35 zeolite although the zeolite has corrugated channels: 18-MR cages with 10-MR pore-entrance (0.54 nm × 0.57 nm). Almost no isomerization of 4,4′-DIPB occurs at the acid sites on external and internal surfaces of STF zeolite as shown in Fig. 11. These results indicate that the isopropylation of BP occurs inside their channels of SSZ-35 zeolite, and that low selectivity for 4,4′-DIPB is due to non-selective formation of DIPB isomers because the channels are too large for the selective formation of 4,4′-DIPB. However, the selectivity for 4,4′-DIPB, compared to its equilibrium composition, over SSZ-35 zeolite suggests that the channels have some shape-selective nature due to the steric restriction by the channels.

It is interesting how bulky DIPB isomers, such as 2,*x*′-, 3,4′-, and 3,3′-DIPB can diffuse out from the SSZ-35 channels. However, we currently have not enough explanation on the catalytic properties of SSZ-35 zeolite. Further research are necessary for these aspects.

4. Conclusion

The isopropylation of biphenyl was examined over SSZ-55, SSZ-42, L, and SSZ-35 zeolites with ATS, IFR, LTL, and STF topologies, which have one-dimensional corrugated channels. The selectivities for 4,4′-DIPB over these zeolites were in the range of 10–40%: they were much lower than that of MOR although these zeolites have similar size of pore-entrance. These

differences are due to the channel structures. SSZ-55, SSZ-42, L, and SSZ-35 zeolites have one-dimensional corrugated channels; however, MOR has one-dimensional straight channels with side pockets. These results show that the shape-selective catalysis of zeolites in the isopropylation of BP was governed by the channels structures as well as size of the pore-entrances.

Further aspects on the shape-selective catalysis on zeolite structures are under investigation. The details will be discussed in near future.

Acknowledgement

A part of this work was financially supported by a Grant-in Aid for Scientific Research (B) 16310056 and 19061107, the Japan Society for the Promotion of Science (JSPS), and by Research Project under the Japan-Korea Basic Scientific Cooperation Program, JSPS and Korea Science and Engineering Foundation (KOSEF; Grant No. F01-2004-000-10510-0). The authors also appreciate the gift of SSZ-35 zeolite from Dr. Megumu Inaba of Advanced National Institute of Science and Technology (AIST).

Appendix A. Supplementary data

Supplementary data associated with this article can be found, in the online version, at doi:10.1016/j.molcata.2007.09.020.

References

[1] Y. Sugi, Y. Kubota, in: J.J. Spivey (Ed.), Catalysis, Specialist Periodical Report, vol. 13, Royal Soc. Chem., 1997, pp. 55–84 (Chapter 3).
[2] Y. Sugi, Korean J. Chem. Eng. 17 (2000) 1.
[3] Y. Sugi, Y. Kubota, T. Hanaoka, T. Matsuzaki, Catal. Survey Jpn. 5 (2001) 43.
[4] Y. Sugi, K. Komura, J.-H. Kim, J. Korean Ind. Eng. Chem. 17 (2006) 235.
[5] T. Matsuzaki, Y. Sugi, T. Hanaoka, K. Takeuchi, H. Arakawa, T. Tokoro, G. Takeuchi, Chem. Express 4 (1989) 413.
[6] Y. Sugi, T. Matsuzaki, T. Hanaoka, Y. Kubota, J.-H. Kim, X. Tu, M. Matsumoto, Catal. Lett. 27 (1994) 315.
[7] Y. Sugi, S. Tawada, T. Sugimura, Y. Kubota, T. Hanaoka, T. Matsuzaki, K. Nakajima, K. Kunimori, Appl. Catal. A: Gen. 189 (1999) 251.
[8] R.K. Ahedi, S. Tawada, Y. Kubota, Y. Sugi, J.-H. Kim, J. Mol. Catal. A: Chem. 197 (2003) 133.
[9] A. Ito, H. Maekawa, H. Kawagoe, K. Komura, Y. Kubota, Y. Sugi, Bull. Chem. Soc. Jpn. 80 (2007) 215.
[10] M. Bandyopadhyay, R. Bandyopadhyay, S. Tawada, Y. Kubota, Y. Sugi, Appl. Catal. A: Gen. 225 (2002) 51.
[11] H. Maekawa, S.K. Saha, S.A.R. Mulla, S.B. Waghmode, K. Komura, Y. Kubota, Y. Sugi, J. Mol. Catal. A: Chem. 263 (2007) 238.
[12] H. Maekawa, C. Naitoh, K. Nakagawa, A. Iida, K. Komura, Y. Kubota, Y. Sugi, J.-H. Kim, G. Seo, J. Mol. Catal. A: Chem. 274 (2007) 24.
[13] S.K. Saha, S.B. Waghmode, H. Maekawa, R. Kawase, K. Komura, Y. Kubota, Y. Sugi, Microporous Mesoporous Mater. 81 (2005) 277.
[14] S.K. Saha, H. Maekawa, S.B. Waghmode, S.A.R. Mulla, K. Komura, Y. Kubota, Y. Sugi, S.-J. Cho, Mater. Trans. 46 (2005) 2659.
[15] International Zeolite Association, http://www.iza-online.org/.
[16] C.-Y. Chen, S.I. Zones, US Patent 6,468,501 (2002).
[17] S. Elomari, T.V. Harris, US Patent 6,475,463 (2002).
[18] S.A. Elomari, S.I. Zones, Stud. Surf. Sci. Catal. 135 (2001) 479.
[19] M.G. Wu, M.W. Deem, S. Elomari, R.C. Medrud, S.I. Zones, T. Maesen, C. Kibby, C.Y. Chen, I.Y. Chan, J. Phys. Chem. B 106 (2002) 264.
[20] S.I. Zones, US Patent 5,653,956 (1997).
[21] C.Y. Chen, L.W. Finger, R.C. Medrud, P.A. Crozier, I.Y. Chan, T.V. Harris, S.I. Zones, Chem. Commun. (1997) 1773.
[22] C.Y. Chen, S.I. Zones, L.T. Yuen, T.V. Harris, S.A. Elomari, Proceedings of the 12th International Zeolite Conference III 1945, 2001.
[23] C.Y. Chen, L.W. Finger, R.C. Medrud, C.L. Kibby, P.A. Crozier, I.Y. Chan, T.V. Harris, L.W. Beck, I. Zones, Chem. Eur. J. 4 (1998) 1312.
[24] Y. Nakagawa, US Patent 5,316,753 (1994).
[25] R.F. Lobo, M. Tsapatsis, C.C. Freyhardt, I. Chan, C.Y. Chen, S.I. Zones, M.E. Davis, J. Am. Chem. Soc. 119 (1997) 3732.
[26] P. Wagner, S.I. Zones, M.E. Davis, R.C. Medrud, Angew. Chem. Int. Ed. 38 (1999) 1269.
[27] P. Wagner, Y. Nakagawa, G.S. Lee, M.E. Davis, S. Elomari, R.C. Medrud, S.I. Zones, J. Am. Chem. Soc. 122 (2000) 263.
[28] Y. Kurata, T. Hanaoka, H. Hamada, Stud. Surf. Sci. Catal. 135 (2001) 366.
[29] M. Inaba, K. Murata, M. Saito, I. Takahara, N. Mimura, H. Hamada, Y. Kurata, Bull. Chem. Soc. Jpn. 77 (2004) 381.
[30] G. Takeuchi, H. Okazaki, T. Kito, Y. Sugi, T. Matsuzaki, Sekiyu Gakkaishi 34 (1991) 242.
[31] Y. Sugi, H. Maekawa, Y. Hasegawa, A. Ito, R. Asai, D. Yamamoto, K. Komura, Y. Kubota, J.-H. Kim, G. Seo, Catal. Today, in press.
[32] Y. Sugi, H. Maekawa, S.A.R. Mulla, A. Ito, C. Naitoh, K. Nakagawa, K. Komura, Y. Kubota, J.-H. Kim, G. Seo, Bull. Chem. Soc. Jpn. 80 (2007) 1418.